Electronic Supplementary Information

High-throughput screening of B/N-doped graphene supported single atom catalysts for nitrogen reduction reaction

Ning Cao[1], Nan Zhang[2], Ke Wang[1], Keping Yan[1, 3], Pengfei Xie[*1,3]

[1] College of Chemical and Biological Engineering, Zhejiang University, Hangzhou 310027, China

[2] State Key Laboratory of Coordination Chemistry, School of Chemistry and Chemical Engineering, Nanjing University, Nanjing 210008, China

[3] Shanxi-Zheda Institute of Advanced Materials and Chemical Engineering, Taiyuan, 030032, China

Corresponding Email:

pfxie@zju.edu.cn

Table 1. Calculated binding energies (E_b) for all TM_1-B_2N_2/G catalysts. And the difference between binding energies and cohesive energies (E_c) for all TM_1-B_2N_2/G catalysts.

	E_b (eV)			E_b - E_c (eV)		
	TM_1-B_2N_2/ G-1	TM_1-B_2N_2/ G-2	TM_1-B_2N_2/ G-3	TM_1-B_2N_2/ G-1	TM_1-B_2N_2/ G-2	TM_1-B_2N_2/ G-3
Sc	-5.06	-7.82	-4.25	-0.15	-2.91	0.66
Ti	-5.71	-7.92	-5.29	-0.89	-1.32	1.31
V	-5.17	-7.07	-4.77	-1.46	-0.45	1.85
Cr	-5.04	-6.78	-4.44	-0.01	-1.75	0.59
Mn	-3.97	-5.40	-3.93	-0.19	-1.62	-0.15
Fe	-4.79	-6.25	-5.01	0.09	-1.37	-0.13
Co	-5.13	-6.40	-5.22	-0.02	-1.29	-0.11
Ni	-5.40	-6.69	-5.57	-0.30	-1.59	-0.47
Cu	-3.96	-5.36	-2.88	-0.46	-1.86	0.62
Zn	-1.38	-3.56	-0.71	-1.16	-3.33	-0.48

Table 2. Summary of adsorption energies of *N_2 (E_{ad}) for all TM_1-B_2N_2/G catalysts.

	End-on (eV)			Side-on (eV)		
	TM_1-B_2N_2/ G-1	TM_1-B_2N_2/ G-2	TM_1-B_2N_2/ G-3	TM_1-B_2N_2/ G-1	TM_1-B_2N_2/ G-2	TM_1-B_2N_2/ G-3
Sc	-0.49	-0.72	-0.62	-0.30	-0.59	-0.47
Ti	-0.85	-1.06	-0.82	-0.46	-1.12	-0.63
V	-0.85	-1.03	-0.89	-0.63	-0.86	-0.54
Cr	-0.95	-0.97	-0.94	-0.40	-0.65	-0.46
Mn	-1.03	-0.76	-0.55	-0.75	-0.43	-0.09
Fe	-1.39	-0.92	-0.50	-0.63	-0.47	-0.20
Co	-1.47	-0.91	-0.71	-0.83	-0.33	-0.45
Ni	-0.88	-0.63	-0.41	-0.32	-0.22	-0.08
Cu	-0.36	-0.26	-0.14	-0.34	-0.08	-0.11
Zn	-0.43	-0.18	-0.08	-0.40	-0.16	-0.07

Table 3. Summary of adsorption free energies of *N$_2$ (G_{ad}) for all TM$_1$-B$_2$N$_2$/G catalysts.

	End-on (eV)			Side-on (eV)		
	TM$_1$-B$_2$N$_2$/ G-1	TM$_1$-B$_2$N$_2$/ G-2	TM$_1$-B$_2$N$_2$/ G-3	TM$_1$-B$_2$N$_2$/ G-1	TM$_1$-B$_2$N$_2$/ G-2	TM$_1$-B$_2$N$_2$/ G-3
Sc	-0.04	-0.29	-0.20	0.13	-0.19	-0.09
Ti	-0.38	-0.62	-0.39	-0.04	-0.66	-0.18
V	-0.39	-0.57	-0.43	-0.19	-0.40	-0.10
Cr	-0.48	-0.49	-0.48	-0.06	-0.18	-0.04
Mn	-0.54	-0.31	-0.12	-0.23	0.00	0.27
Fe	-0.89	-0.46	-0.06	-0.15	0.00	0.25
Co	-0.95	-0.44	-0.24	-0.36	0.08	0.02
Ni	-0.40	-0.17	0.03	0.06	0.20	0.34
Cu	0.00	0.19	0.25	0.12	0.27	0.27
Zn	-0.09	0.22	0.32	0.02	0.22	0.33

Table 4. The N≡N bond lengths during N$_2$ activation for all catalysts.

	End-on (Å)			Side-on (Å)		
	TM$_1$-B$_2$N$_2$/ G-1	TM$_1$-B$_2$N$_2$/ G-2	TM$_1$-B$_2$N$_2$/ G-3	TM$_1$-B$_2$N$_2$/ G-1	TM$_1$-B$_2$N$_2$/ G-2	TM$_1$-B$_2$N$_2$/ G-3
Sc	1.128	1.128	1.128	1.153	1.150	1.149
Ti	1.134	1.133	1.127	1.159	1.173	1.163
V	1.138	1.136	1.134	1.180	1.173	1.163
Cr	1.137	1.134	1.132	1.205	1.167	1.148
Mn	1.138	1.133	1.126	1.236	1.163	1.143
Fe	1.140	1.133	1.128	1.177	1.156	1.163
Co	1.138	1.132	1.132	1.177	1.149	1.165
Ni	1.131	1.130	1.124	1.136	1.148	1.140
Cu	1.114	1.123	1.114	1.114	1.114	1.114
Zn	1.114	1.114	1.114	1.114	1.114	1.114
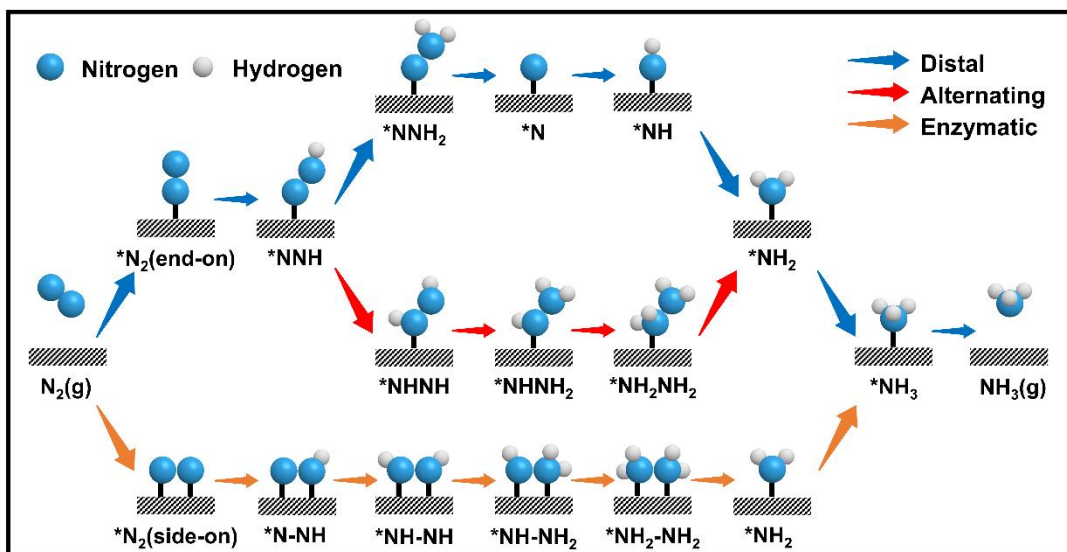
Figure 1. The reaction mechanism of NRR.

Table 5. Free energy changes for the first PCET (eV) throughout the NRR process.

	*N$_2$(End-on)	*NNH		*N$_2$(Side-on)	*N-NH	
	TM$_1$-B$_2$N$_2$/ G-1	TM$_1$-B$_2$N$_2$/ G-2	TM$_1$-B$_2$N$_2$/ G-3	TM$_1$-B$_2$N$_2$/ G-1	TM$_1$-B$_2$N$_2$/ G-2	TM$_1$-B$_2$N$_2$/ G-3
Sc	1.54	1.10	1.14	0.85	0.51	0.64
Ti	1.07	0.94	1.12	0.28	0.58	0.56
V	0.49	0.75	0.70	0.06	0.58	0.48
Cr	0.55	0.74	0.82	0.41	0.54	0.47
Mn	0.64	0.74	1.04	1.26	0.90	0.79
Fe	0.71	0.87	1.10	0.97	1.21	0.74
Co	1.04	0.88	1.28	1.19	0.84	1.18
Ni	0.81	0.90	1.53	0.92	1.10	1.78
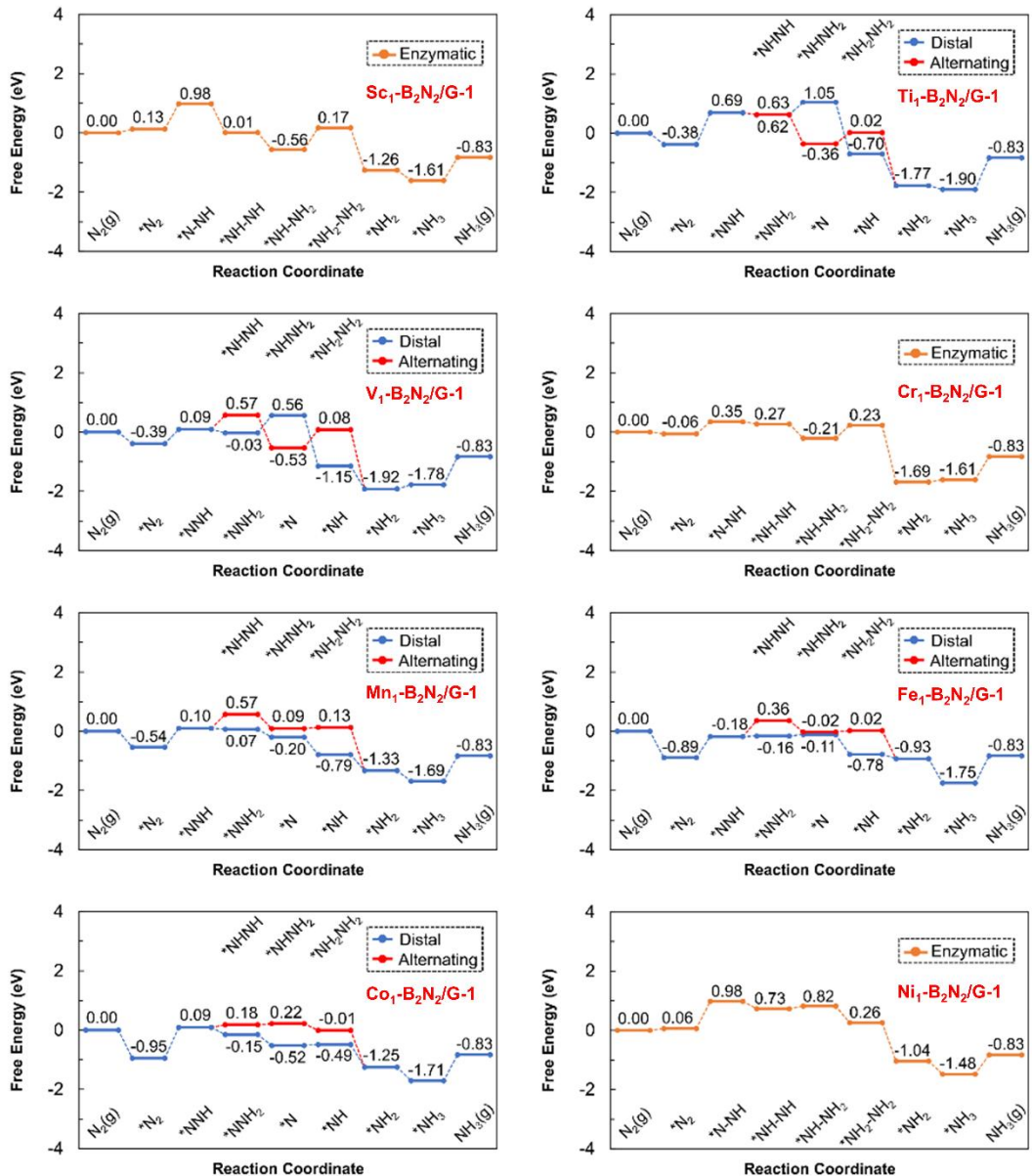
Figure 2. Optimal NRR mechanism of TM_1-B_2N_2G-1 catalysts and their corresponding values of free energy change.
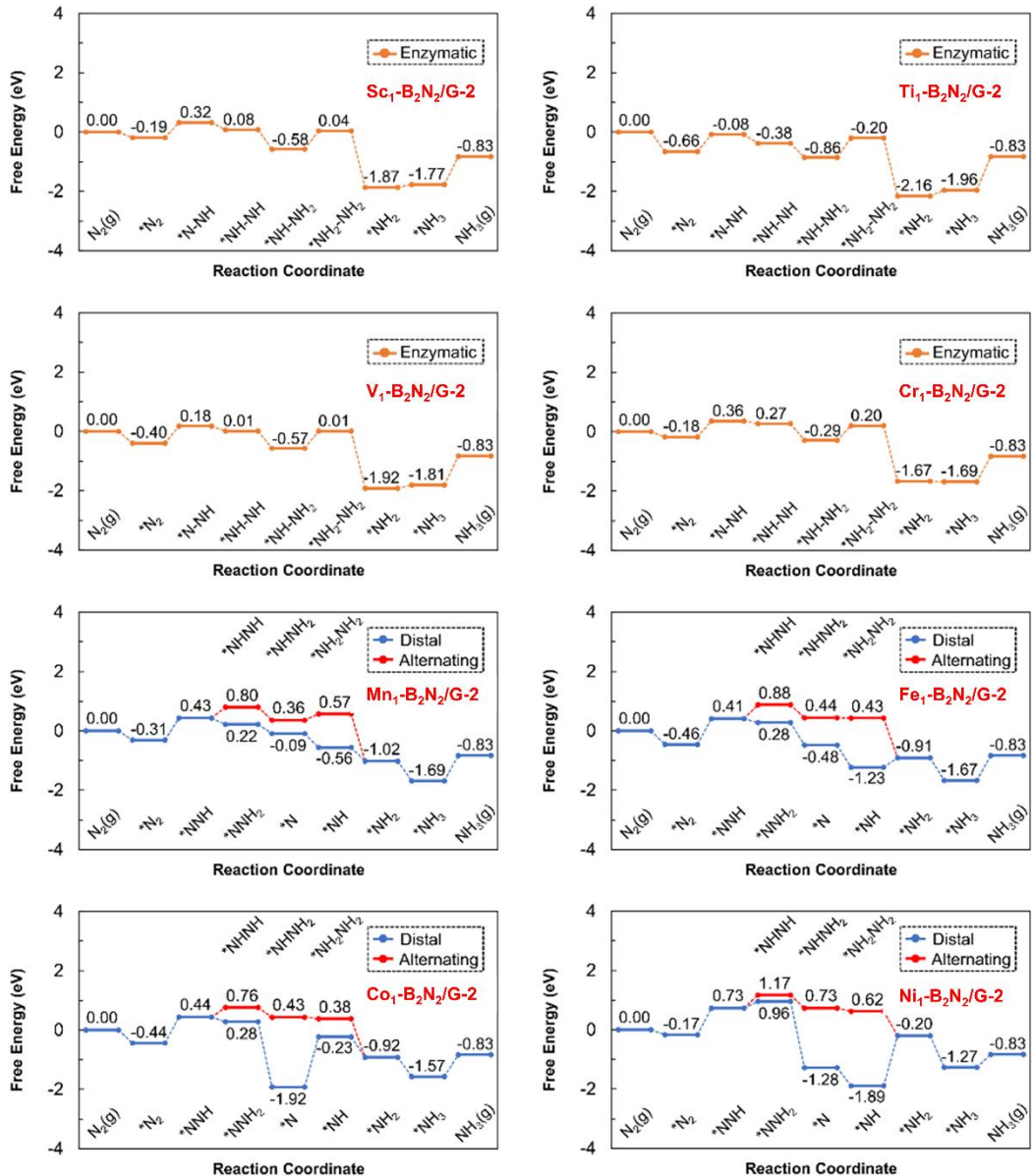
Figure 3. Optimal NRR mechanism of TM_1-B_2N_2G-2 catalysts and their corresponding values of free energy change.
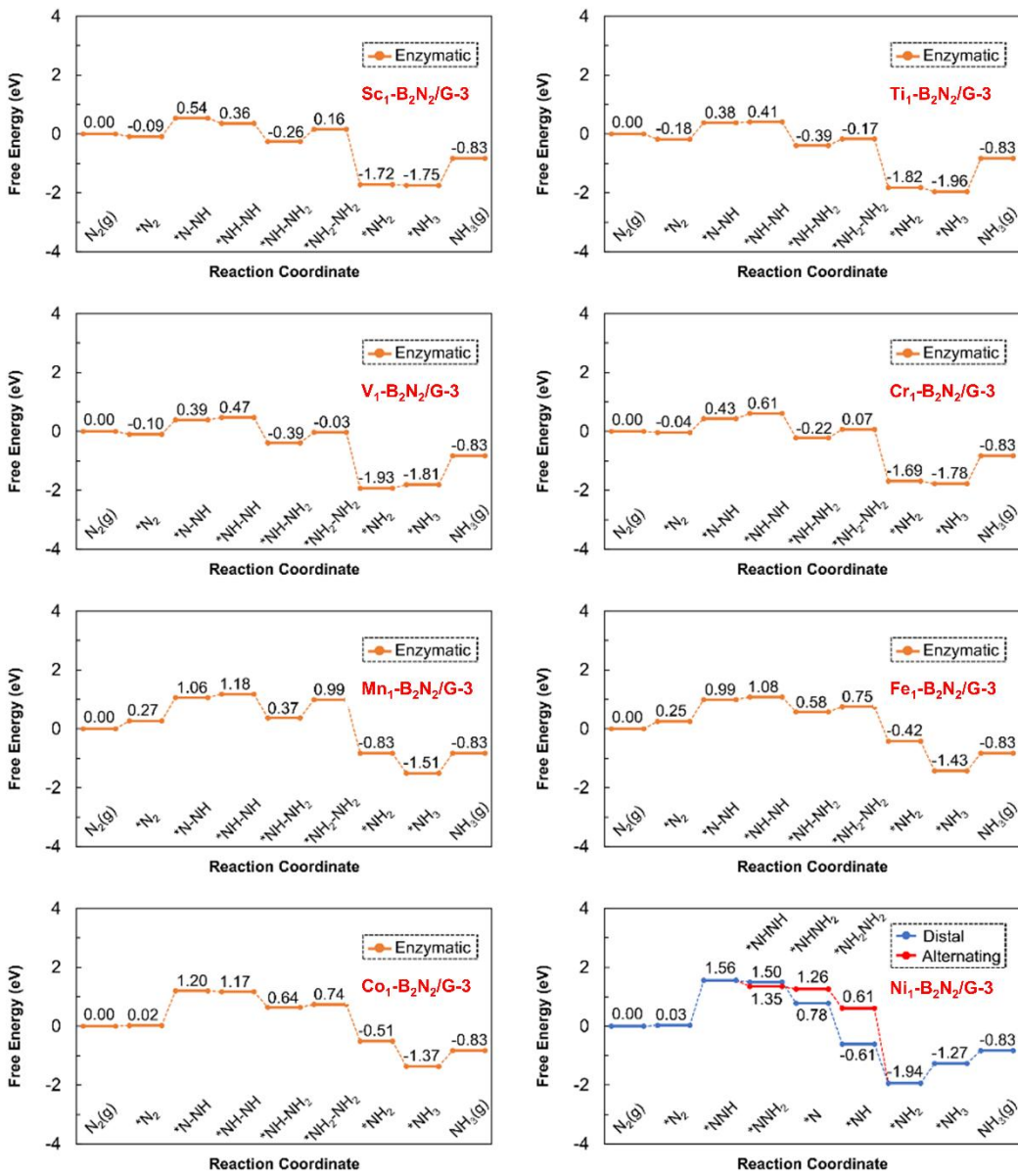
Figure 4. Optimal NRR mechanism of TM_1-B_2N_2G-3 catalysts and their

corresponding values of free energy change.

Table 6. Limiting potentials (U_L) for all reaction mechanisms throughout the NRR process.

U_L(V)	Distal	Alternating	Enzymatic
Sc_1-B_2N_2/G-1	-1.54	-1.54	-0.85
Ti_1-B_2N_2/G-1	-1.07	-1.07	-1.34
V_1-B_2N_2/G-1	-0.59	-0.61	-0.77
Cr_1-B_2N_2/G-1	-0.55	-0.55	-0.43
Mn_1-B_2N_2/G-1	-0.64	-0.64	-1.26
Fe_1-B_2N_2/G-1	-0.71	-0.71	-0.97
Co_1-B_2N_2/G-1	-1.04	-1.04	-1.19
Ni_1-B_2N_2/G-1	-0.94	-1.27	-0.91
Sc_1-B_2N_2/G-2	-1.10	-1.10	-0.62
Ti_1-B_2N_2/G-2	-0.94	-0.94	-0.67
V_1-B_2N_2/G-2	-0.75	-0.75	-0.58
Cr_1-B_2N_2/G-2	-0.74	-0.74	-0.54
Mn_1-B_2N_2/G-2	-0.74	-0.74	-0.90
Fe_1-B_2N_2/G-2	-0.87	-0.87	-1.21
Co_1-B_2N_2/G-2	-1.69	-0.88	-0.84
Ni_1-B_2N_2/G-2	-1.69	-0.90	-1.10
Sc_1-B_2N_2/G-3	-1.14	-1.14	-0.64
Ti_1-B_2N_2/G-3	-1.12	-1.12	-0.56
V_1-B_2N_2/G-3	-0.70	-0.70	-0.48
Cr_1-B_2N_2/G-3	-0.82	-0.82	-0.47
Mn_1-B_2N_2/G-3	-1.04	-1.04	-0.79
Fe_1-B_2N_2/G-3	-1.10	-1.10	-0.74
Co_1-B_2N_2/G-3	-1.28	-1.28	-1.18
Ni_1-B_2N_2/G-3	-1.53	-1.53	-1.78
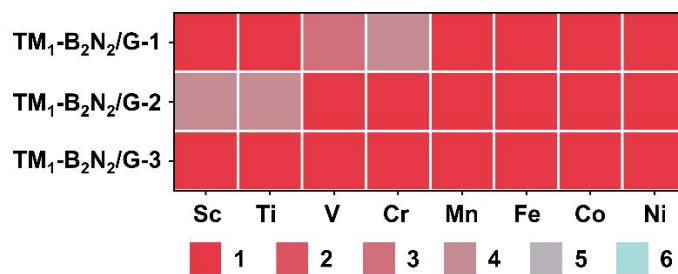
Figure 5. Potential-determining steps in the optimal NRR mechanism for all TM_1-B_2N_2/G catalysts.

Table 7. Optimal limiting potentials for all catalysts.

$U_L(V)$	TM$_1$-B$_2$N$_2$/G-1	TM$_1$-B$_2$N$_2$/G-2	TM$_1$-B$_2$N$_2$/G-3
Sc	-0.85	-0.62	-0.64
Ti	-1.07	-0.67	-0.56
V	-0.59	-0.58	-0.48
Cr	-0.43	-0.54	-0.47
Mn	-0.64	-0.74	-0.79
Fe	-0.71	-0.87	-0.74
Co	-1.04	-0.84	-1.18
Ni	-0.92	-0.90	-1.53
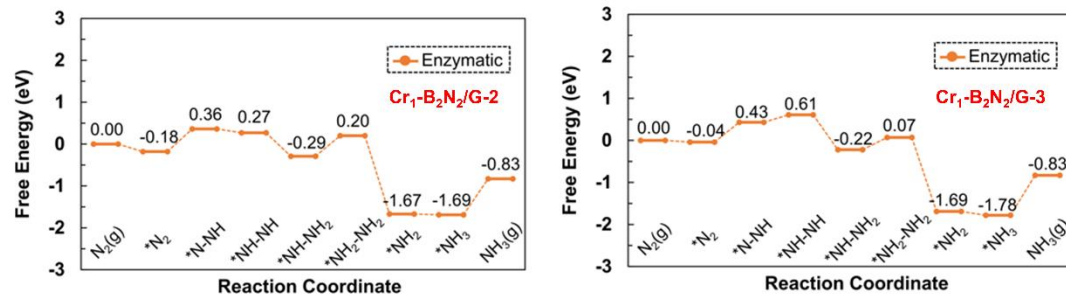
Figure S. Optimal NRR mechanism of Cr$_1$-B$_2$N$_2$G-2 and Cr$_1$-B$_2$N$_2$G-3 catalysts and their corresponding values of free energy change.
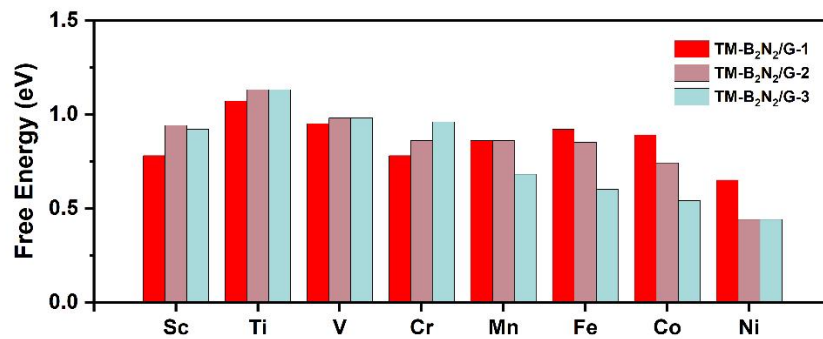
Figure 7. Values of free energy change for the second NH$_3$ desorption.

Cr$_1$-B$_2$N$_2$/G-1   Cr$_1$-B$_2$N$_2$/G-2   Cr$_1$-B$_2$N$_2$/G-3
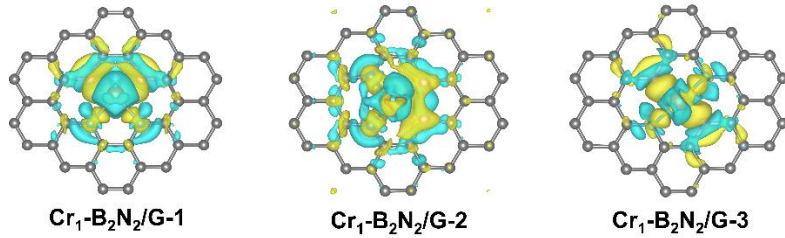
Figure 8. The charge density difference of Cr anchored to the different B$_2$N$_2$/G supports. The yellow and cyan isosurfaces represent charge accumulation and depletion in the space. The isosurface value was set to be 0.002 e·Å^{-3}.

Cr$_1$-B$_2$N$_2$/G-1   Cr$_1$-B$_2$N$_2$/G-2   Cr$_1$-B$_2$N$_2$/G-3
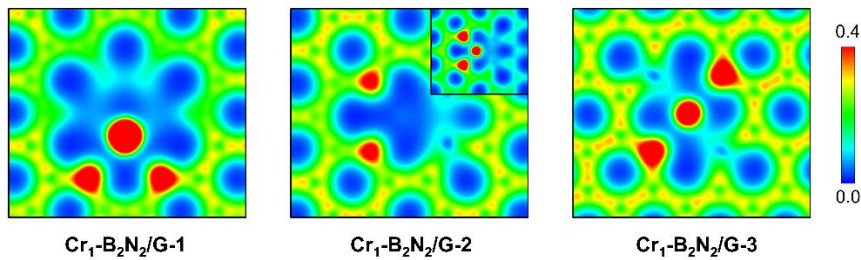
Figure 9. The charge density of different Cr$_1$-B$_2$N$_2$/G catalysts

Table 8. Electron localization function (ELF) values between Cr-N-B for all catalysts.

	TM$_1$-B$_2$N$_2$/G-1	TM$_1$-B$_2$N$_2$/G-2	TM$_1$-B$_2$N$_2$/G-3
Cr-B	0.387	0.308	0.645
Cr-N	0.794	0.734	0.778
B-N	0.094	0.028	0.095/0.037
B-B	0.037	0.814	---
N-N	0.020	0.035	---

Table 9. Bader charge transferred from the supports to the transition metal during the

metal-support interaction (e⁻).

	TM$_1$-B$_2$N$_2$/G-1	TM$_1$-B$_2$N$_2$/G-2	TM$_1$-B$_2$N$_2$/G-3
Sc	1.666	1.469	1.540
Ti	1.551	1.379	1.393
V	1.277	1.119	1.160
Cr	1.156	0.862	0.943
Mn	1.099	0.801	0.815
Fe	0.723	0.581	0.468
Co	0.624	0.344	0.308
Ni	0.496	0.303	0.179
Cu	0.326	0.496	0.249
Zn	0.702	0.366	0.559

Table 10. Bader charge transferred from the catalyst to N$_2$ during the N$_2$ activation (e⁻).

	End-on			Side-on		
	TM$_1$-B$_2$N$_2$/ G-1	TM$_1$-B$_2$N$_2$/ G-2	TM$_1$-B$_2$N$_2$/ G-3	TM$_1$-B$_2$N$_2$/ G-1	TM$_1$-B$_2$N$_2$/ G-2	TM$_1$-B$_2$N$_2$/ G-3
Sc	0.221	0.224	0.202	0.383	0.355	0.347
Ti	0.287	0.289	0.188	0.392	0.500	0.405
V	0.329	0.313	0.267	0.498	0.479	0.384
Cr	0.315	0.286	0.247	0.568	0.413	0.458
Mn	0.311	0.273	0.155	0.501	0.396	0.236
Fe	0.328	0.262	0.186	0.423	0.323	0.345
Co	0.283	0.235	0.224	0.396	0.251	0.340
Ni	0.218	0.238	0.133	0.362	0.242	0.166
Cu	0.018	0.151	0.014	0.010	0.013	0.015
Zn	0.016	0.010	0.021	0.014	0.011	0.021
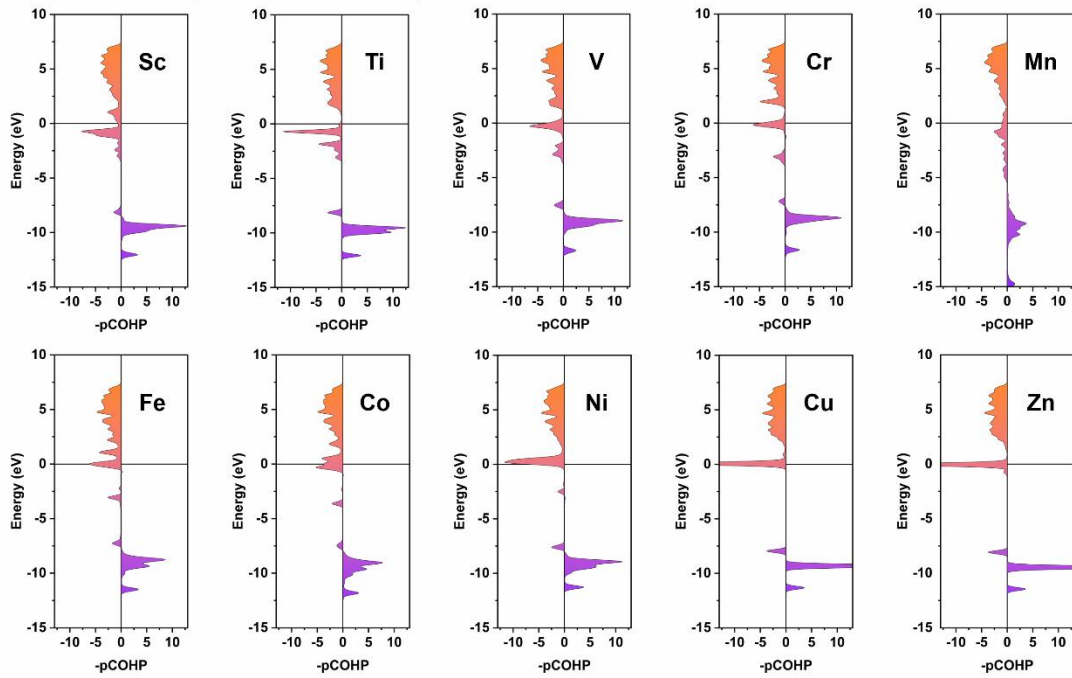
Figure 10. The partial Crystal Orbital Hamiltonian Population (pCOHP) of $N\equiv N$

bonds in TM_1-B_2N_2/G-1 catalysts adsorbed with N_2 in Side-on mode.
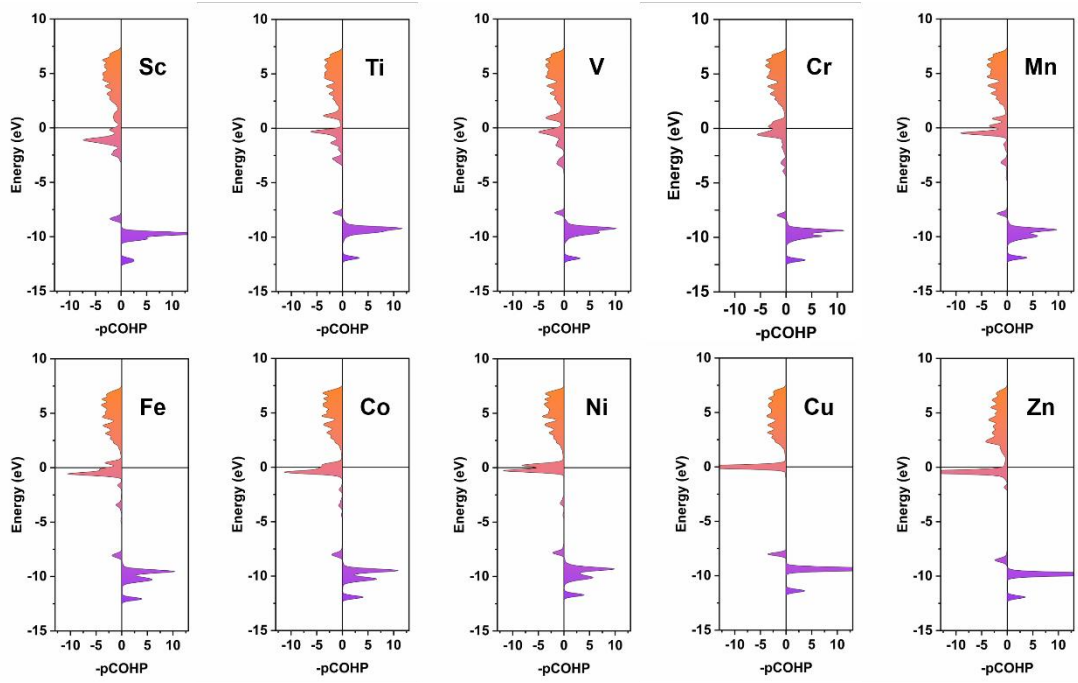
**Figure 11.** The pCOHP of N≡N bonds in TM_1-B_2N_2/G-2 catalysts adsorbed with N_2 in Side-on mode.
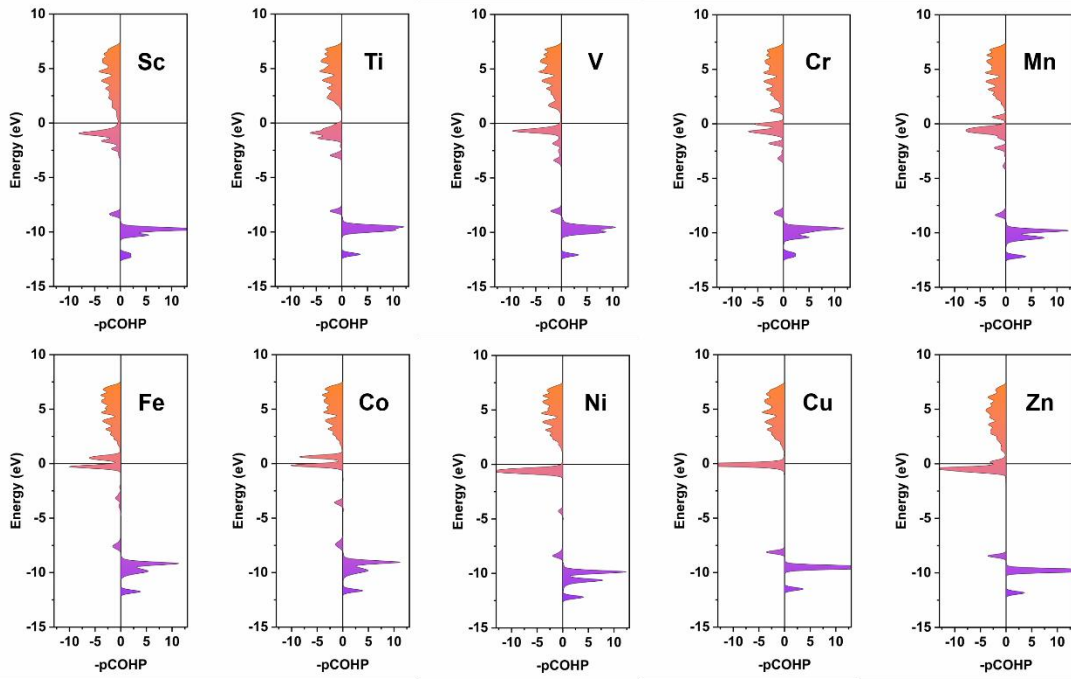
Figure 12. The pCOHP of N≡N bonds in $TM_1-B_2N_2/G-3$ catalysts adsorbed with N_2 in Side-on mode.
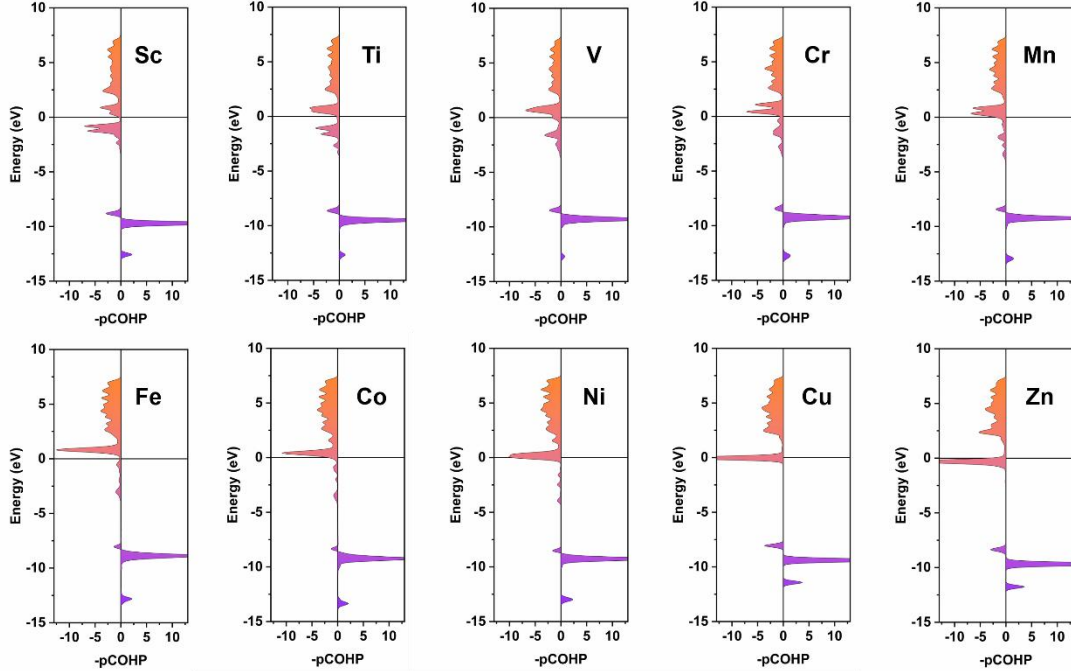
Figure 13. The pCOHP of N≡N bonds in $TM_1-B_2N_2/G-1$ catalysts adsorbed with N_2 in End-on mode.
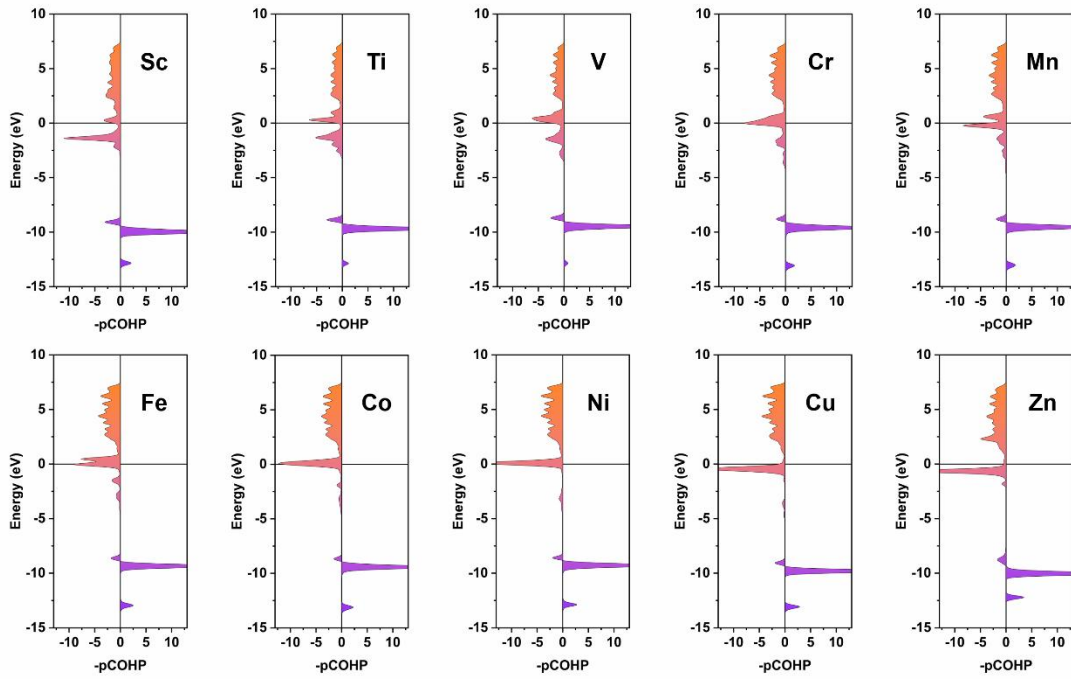
Figure 14. The pCOHP of N≡N bonds in TM_1-B_2N_2/G-2 catalysts adsorbed with N_2 in End-on mode.
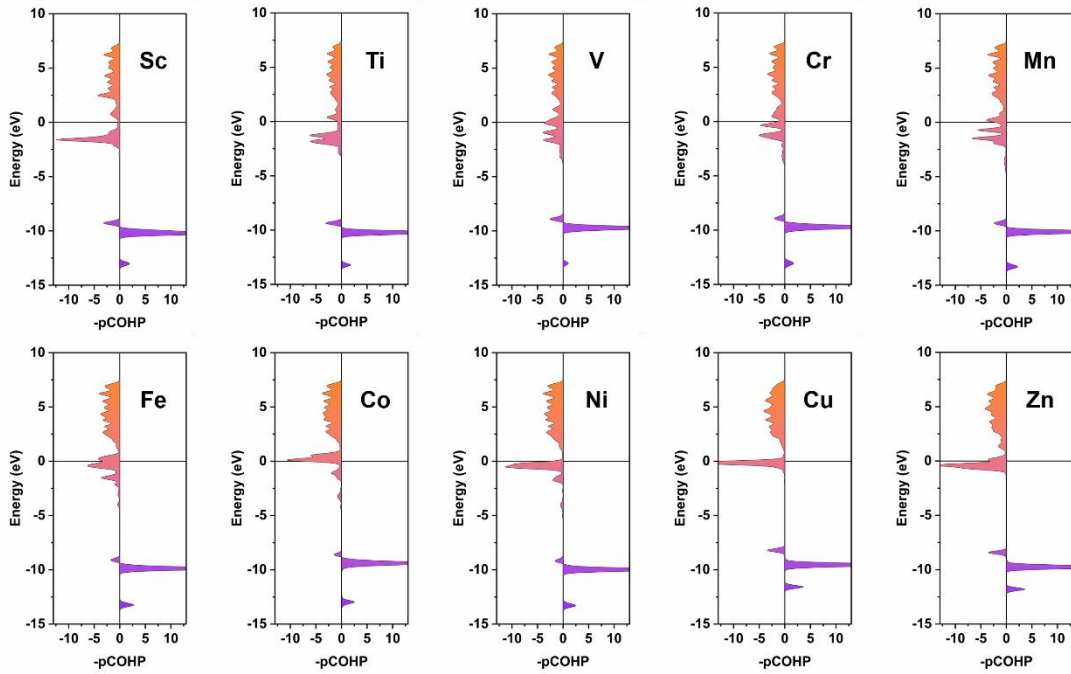
Figure 15. The pCOHP of N≡N bonds in TM_1-B_2N_2/G-3 catalysts adsorbed with N_2 in End-on mode.
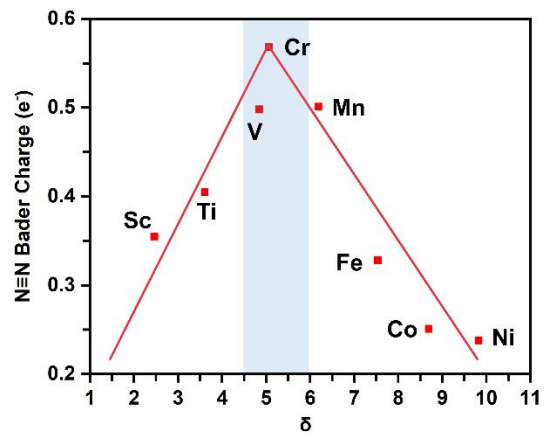
Figure 16. The volcano plot of N≡N Bader charge versus the valence electron

number (δ) of transition metal single atom.